Asymptotic Giant Branch Stars
T. Le Bertre, A. Lèbre and C. Waelkens, eds.
I.A.U. Symposium 191, 1999

ISO results on circumstellar envelopes

M. J. Barlow
Dept. of Physics & Astronomy, University College London, Gower St., London WC1E 6BT, U.K.

Abstract.
This review covers spectroscopic results obtained with ISO on molecular and atomic line emission from the circumstellar envelopes of oxygen-rich AGB stars and post-AGB objects and from cool supergiant stars. As well as the SWS detection of the 4.27-μm CO_2 band in absorption and emission from cool star envelopes, several new emission bands which have been detected in SWS spectra between 13.9 and 16.2 μm have been identified with CO_2 bands. Strong H_2O line emission has been observed in the LWS and SWS spectra of high mass loss rate O-rich AGB and M supergiant stars, confirming the predicted importance of this molecule as a coolant in their outflows. The proposed infrared radiative pump mechanism for circumstellar OH masers has been directly confirmed for the first time via measurements for several stars of the OH infrared pumping lines between 34.6 μm and 163 μm. Water vapour emission lines are not present in the spectra of O-rich post-AGB objects, having been replaced by broad emission features at 43 and 62 μm due to crystalline water ice that has condensed in the very cool outflows.

1. Introduction

In this review I will concentrate on ISO observations of atomic and molecular species around oxygen-rich cool evolved stars, although some discussion is included of observations of water ice emission bands. Space limitations preclude more than a passing mention of ISO results for carbon-rich objects – reviews of results on C-rich objects have been presented by Barlow (1998a) and by Cernicharo (1998). A companion review (Waters & Molster, this volume) describes ISO observations of solid-state dust features from evolved stars.

The plan of this review will be to concentrate first on results pertaining to smaller circumstellar radii (i.e. from warm material, absorbing or emitting at SWS infrared wavelengths), followed by a discussion of observations of species located at larger circumstellar radii (i.e. cooler material, emitting at longer, LWS, wavelengths).

2. ISO SWS observations of molecules in cool star envelopes

Prior to the launch of ISO, telluric absorption lines arising high in our own atmosphere had prevented observations of many of the bands of H_2O and CO_2 that

had been predicted to be strong in cool star spectra. Justtanont et al. (1996) presented the 2.4–45-μm SWS grating spectrum of the highly evolved M supergiant NML Cyg, obtained with a resolving power (depending on wavelength) of between 700 and 1400. The 6.2-μm ν_2 (bending mode) ro-vibrational band of H_2O was detected in absorption, together with the 2.7-μm ν_1 and ν_3 stretching bands. The strength of the higher-excitation 2.7-μm absorption band implied that it must originate from a hotter region (with T > 500 K) interior to where the 6.2-μm band absorption originates. Justtanont et al. (1996) also detected for the first time absorption due to the 4.27-μm stretching band of CO_2. The 15.2-μm bending mode band of CO_2 was not detected however. Since they also detected strong absorption in the CO fundamental ro-vibration band at 4.6 μm, Justtanont et al. were able to derive an overall CO/CO_2 column density ratio of 5. From fits to the 2.7-μm H_2O band, they obtained a surprisingly high $^{12}C/^{13}C$ ratio of > 100.

Tsuji et al. (1997) presented similar SWS observations of these bands for the M2-M7 giants β Peg, 30g Her, SW Vir and RT Vir, and for the Mira variable S Vir. Their observations of the 2.7-μm H_2O absorption band could be fitted by a H_2O layer located at about two stellar radii, with an excitation temperature of 1250 K. They also found broad excess absorption at 4.27-μm in the spectra of the M7III stars SW Vir and RT Vir, and in the spectrum of the Mira variable S Vir. This absorption could be fitted by CO_2 columns with excitation temperatures of 750–1250 K, located at a similar radius ($\sim 2R_*$) to that deduced for the water vapour responsible for the 2.7-μm H_2O band.

Justtanont et al. (1998) reported the identification of four new emission lines discovered in the mid-infrared SWS spectra of five AGB stars. The detective story started with the observation of emission features at 13.87 and 16.18 μm, together with a feature at 14.97 μm which could appear in emission or absorption, in low-resolution (R $\sim$ 250) SWS grating spectra of several AGB stars having prominent 13-μm broad dust emission features. At first it was suspected that the new features might be linked to the 13-μm dust band carrier, but further analysis, together with the subsequent acquisition of higher resolution grating and Fabry-Perot SWS spectra of the stars, led to their identification with Q-branch ro-vibrational bands of CO_2. The 14.97-μm band is the fundamental (ground-state) ro-vibrational ν_2 band of CO_2 – it appears in absorption in the spectra of two of the AGB stars (R Cas and W Hya) and in emission in the spectra of RX Boo and EP Aqr. Its appearance in absorption was attributed to the additional presence of hot ν_2 bands of CO_2, with the ensemble of transitions, estimated to arise from material at $\sim$ 1250 K, shifting the absorption peak to a slightly shorter wavelength than for the fundamental band alone. The transitions at 13.87, 15.40 and 16.18 μm (all seen in emission), originate from excited ro-vibrational transitions from levels in the ladder above that responsible for the fundamental 14.97-μm transition. Justtanont et al. estimated typical excitation temperatures of $\sim$ 650 K from the observed relative intensities and estimated that the lines are formed a few stellar radii above the photosphere. These physical parameters are very similar to those derived by Tsuji et al. (1997) for the material inferred to be responsible for the 2.7-μm H_2O and 4.27-μm CO_2 absorption bands observed in the spectrum of the AGB star S Vir.

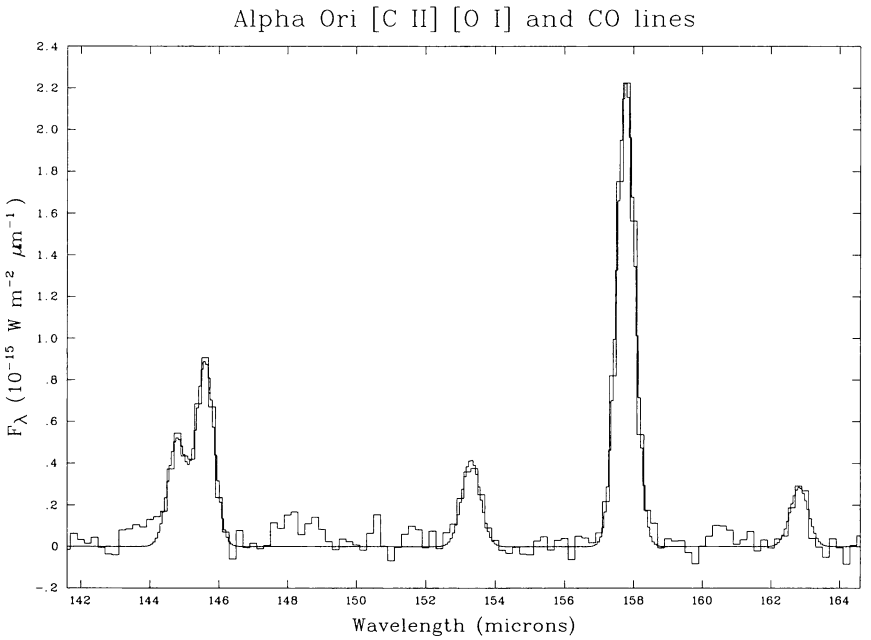

Figure 1. A portion of the background-subtracted and continuum-subtracted LWS spectrum of α Ori. The smooth curve shows Gaussian fits to the observed lines of [O I] and [C II] at 145.5 and 157.7 μm and to the J = 18-17, 17-16 and 16-15 rotational lines of CO at 144.8, 153.3 and 162.8 μm.

3. Infrared fine structure emission lines in the spectra of cool stars

Glassgold & Huggins (1986) and Rodgers & Glassgold (1991) have calculated the ionization structure and energy balance for the wind of the M2Iab supergiant α Ori. Due to the presence of a chromosphere, the recombining wind beyond the chromosphere is predicted to be mainly atomic, with the small amount of carbon that associates into CO eventually being dissociated further out in the wind by the interstellar radiation field. The cooling of the wind was predicted to be dominated by atomic fine structure lines. These predictions were confirmed by the KAO observations of α Ori by Haas & Glassgold (1993), who detected strong [O I] 63.2-μm and moderate [Si II] 34.8-μm emission. Haas et al. (1995) extended these KAO observations to include detections of the same lines from α Sco and α Her as well. Both these M supergiants have B-star companions which are expected to irradiate the cool star winds with photodissociating flux levels much higher than the interstellar value. Justtanont et al. (1998, poster contribution, this conference) have obtained SWS grating spectra of both α Ori and α Sco. In addition to the previously detected 34.8-μm line of [Si II], they also detected the 26.0 and 35.3-μm fine structure lines of [Fe II] from both stars and used the [Fe II] flux ratios to estimate an excitation temperature of 1230 K for the emitting region around α Ori, and 1785 K for α Sco.

https://doi.org/10.1017/S0074180900203276 Published online by Cambridge University Press

The LWS grating spectrum of α Ori (part of which is shown in Fig. 1), obtained by the LWS Consortium just two days before the end of the ISO mission, shows the expected emission from the [O I] 63- and 146-μm lines and the [C II] 158-μm line (after subtraction of the background interstellar component in the latter case), as well as the detection of CO rotational lines extending from 174 μm (J = 15-14) to 130 μm (J= 20-19). Although not as strong as the fine structure lines, the integrated flux of these CO lines means that CO cannot be neglected as a wind coolant. The LWS spectrum of α Sco shows the CO lines to be absent and the [O I] and [C II] lines to have line-to-continuum ratios that are four times higher than in the case of α Ori. These two effects, as well as the higher [Fe II] excitation temperature found by Justtanont et al. (1998, poster contribution, this conference), can be attributed to the additional photodissociation and heating of α Sco's wind by its B-star companion.

Aoki et al. (1998) have reported the detection of [Fe II] 26.0 and 35.3 μm and [Si II] 34.8 μm line emission from the wind of the M6III giant 30g Her. They determined column densities for the emitting Fe^+ and Si^+ ions and, with the assumption of standard solar abundance ratios relative to hydrogen, estimated an emitting region mass of $2–3\times10^{-6}$ $M_\odot$. Aoki et al. (1998a) also detected fine structure lines in their SWS spectra of two carbon stars, with one of them, the C7,2 star TX Psc, showing emission in the [Fe I] 24.0 μm, [S I] 25.2 μm and [Fe II] 26.0 μm lines. The neutral and singly ionized lines of Fe yielded an emitting region mass of 6×10^{-6} $M_\odot$, while the neutral S line yielded an emitting mass estimate of 7×10^{-6} $M_\odot$. The close agreement between these two mass estimates indicates a solar Fe/S ratio, i.e. there seems to be no evidence for depletion of Fe onto dust grains in this carbon star's outflow.

4. UIR band emission from M supergiants

Sylvester et al. (1994) discovered the well-known 8.6- and 11.3-μm UIR bands, usually attributed to aromatic hydrocarbons such as PAHs or HAC complexes, superposed on the broad 10-μm silicate emission features of half a dozen M supergiants in the double cluster h & χ Per. Not only were these the coolest objects from which UIR-band emission had been observed, but M supergiants are oxygen-rich, for which equilibrium condensation theory predicts that all available carbon atoms should be locked up in CO molecules, allowing only oxygen-rich molecules and particles to form. Sylvester et al. interpreted the observed presence of carbon-rich species in terms of a non-equilibrium chemistry model by Beck et al. (1992), whereby chromospheric UV radiation (a) liberates atomic carbon by photodissociating CO molecules, enabling the formation of C-rich species as well as the usual silicates; and (b) provides the photons needed to excite the observed UIR-band emission.

While the 8.6-μm band has only ever been seen in the company of other members of the ensemble of PAH-type UIR bands, the UIR band at 11.3 μm is susceptible to confusion with a narrow crystalline olivine band appearing at the same wavelength. It was therefore desirable to obtain further confirmation of the presence of PAH-type hydrocarbons around these M supergiants by searching for the presence of the well-known PAH bands at 6.2 and 7.7 μm in the SWS spectra of these stars. Tsuji et al. (1998) confirmed the presence of these UIR

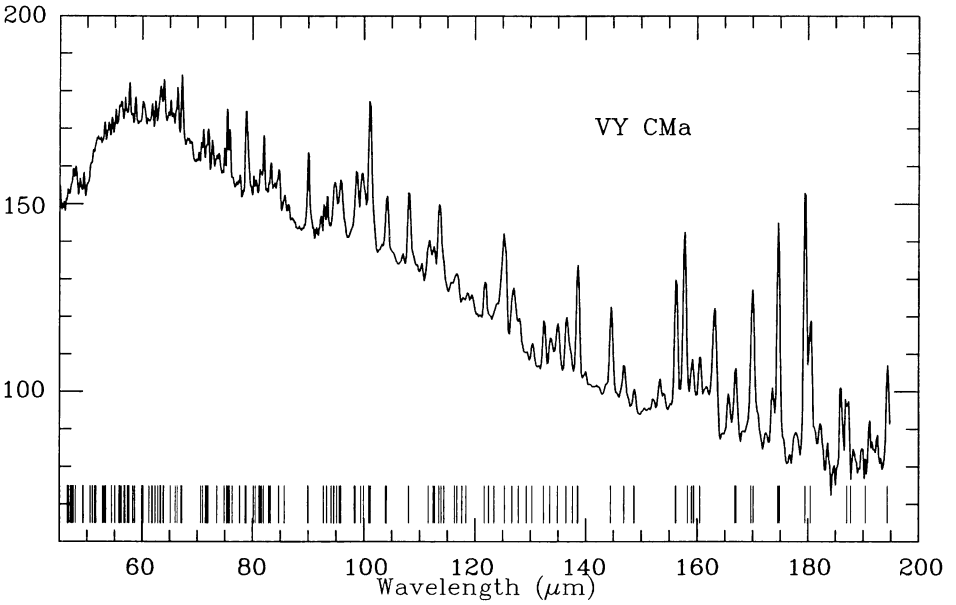

Figure 2. The ISO LWS spectrum of the red supergiant VY CMa. The observed flux (F_λ) has been multiplied by λ^4 to reduce the dynamic range of the vertical axis. Over 100 water lines are detected above the strong dust continuum. The vertical bars below the spectrum indicate the positions of some of the ortho- and para-H_2O rotational lines occurring in the LWS wavelength range.

bands in their SWS spectra of the h & χ Per M supergiants KK Per, FZ Per and HD 14580, while Sylvester (1998) has confirmed their presence in the SWS spectra of several other h & χ Per supergiants, including AD Per.

5. Water vapour line emission and the OH maser pump for cool evolved stars

Because of the huge opacity of the Earth's atmosphere in the far-infrared rotational lines of H_2O, these same lines had never been observed in the spectra of astronomical sources prior to the launch of ISO. Predictions of the importance of these lines as coolants in a variety of astrophysical environments (e.g. Deguchi & Nguyen-Q-Rieu 1990, Neufeld & Kaufman 1993) were quickly confirmed by their widespread detection by ISO. Fig. 2 shows the 43–190-μm LWS grating spectrum of the high luminosity M supergiant VY CMa, whose high mass loss rate wind exhibits a particularly rich water line spectrum, superposed on the strong dust continuum emission from the wind.

Numerous water lines were detected in the 43–190-μm LWS spectrum of the M8e semi-regular variable W Hya by Barlow et al. (1996), and modelled with Sobolev escape probability techniques. While the output spectrum was found

https://doi.org/10.1017/S0074180900203276 Published online by Cambridge University Press

to be sensitive to the mass loss rate and H_2O/H_2 abundance ratio, it was only weakly dependent on the wind temperature gradient and velocity field. Although radiative excitation processes were included in the modelling, the excitation of H_2O was found to be dominated by collisions with H_2. All of the lines observed are optically thick, explaining why so many transitions from high rotational levels are easily detectable. The best fit to the observed water line spectrum was obtained for a mass loss rate of 6×10^{-7} $M_\odot$ yr^{-1}, with H_2O/H_2 ratios of 8×10^{-4} and 3×10^{-4} inside and outside 16 stellar radii, respectively. A distance of 130 pc was adopted by Barlow et al. (1996) – use of the subsequently published HIPPARCOS distance for W Hya of 114 pc would have reduced the derived mass loss rate slightly.

Neufeld et al. (1996) used the SWS Fabry-Perot (R = 30 000) to measure 3 high-J rotational emission lines of water in the 29.8–40.7-μm region of W Hya's spectrum, and also detected 2 further water line features, one in emission and the other in absorption, using the highest resolution grating mode of the SWS (R = 2000). Their modelling of the fluxes observed for these high-J water lines led to a very much larger derived mass loss rate, $(0.5\text{–}3)\times10^{-5}$ $M_\odot$ yr^{-1}, than obtained by Barlow et al. (1996) from their modelling of the lower-J lines observed at longer wavelengths. As pointed out by Neufeld et al., the high mass loss rate which they derived for W Hya is at least a factor of 30 above previous determinations based on mm-wave CO observations. One possible explanation for the discrepancy is that in the innermost regions of the wind, radiative pumping of the ν_2 vibrational level of H_2O from the $\nu = 0$ ground vibrational state, via the absorption of photons in the 6-μm region, may lead to significant overpopulation of high-J rotational levels following the radiative decay back down to the $\nu = 0$ state, thereby causing enhanced emission in the ($\nu = 0$) high-J rotational transitions that are observed in the SWS spectral region.

The many water lines detected in the 43–197 μm LWS grating spectrum of the Mira variable R Cas have been fitted by Truong-Bach et al. (1998) using a circumstellar model that treats in a self-consistent manner the radiative transfer, photodissociation and chemical exchange reactions, together with the heating and cooling processes. Adopting the HIPPARCOS distance of 107 pc and the corresponding stellar radius (1.3 AU) and effective temperature (2400 K) measured by Haniff et al. (1995), Truong-Bach et al. obtained a mass loss rate of 5×10^{-7} $M_\odot$ yr^{-1} from their fit to the observed water line spectrum of R Cas, very similar to the mass loss rate derived for W Hya by Barlow et al. (1996). The H_2O/H_2 abundance ratio was again found to be constant out to a certain radius (20 R_* in this case), beyond which it falls by a factor of three.

Photochemical models (e.g. Huggins & Glassgold 1982) predict that H_2O should be photodissociated by the interstellar radiation field into OH + H at large circumstellar radii. Elitzur, Goldreich & Scoville (1976; EGS) worked out a detailed radiative pump mechanism for OH/IR stars whose maser emission is dominated by the 1612 MHz satellite transition within the J = 3/2 $^2\Pi_{3/2}$ ground state of OH. Their predicted excitation pathway is shown in Fig. 3. The ground $^2\Pi_{3/2}$ J=3/2 state is excited to the $^2\Pi_{1/2}$ J=5/2 state by 34.6-μm line absorption – the preferred decay from there is to the $^2\Pi_{1/2}$ J=3/2 state, with emission at 98.7 μm. The next preferred stage is decay to the $^2\Pi_{1/2}$ J=1/2 state, with emission at 163.2 μm, and finally there is a decay back to

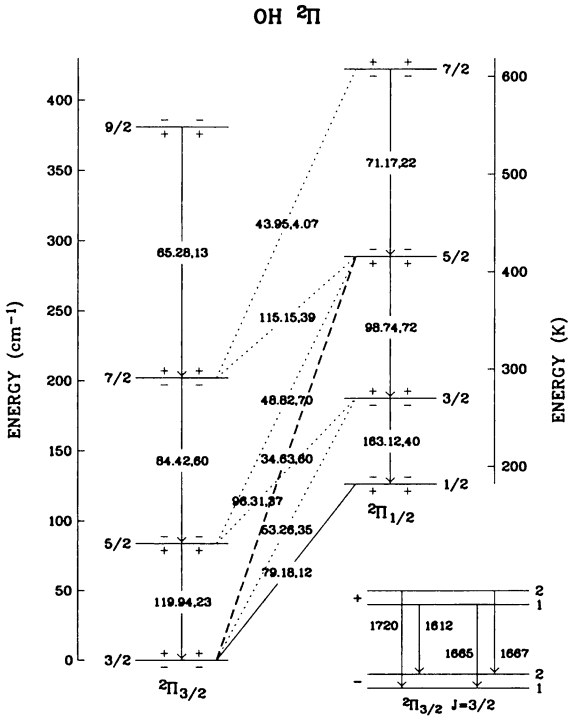

Figure 3. The low-lying energy levels of OH, showing the transitions involved in the maser pumping scheme. The maser action arises from transitions within the J = 3/2 $^2\Pi_{3/2}$ ground state.

the $^2\Pi_{3/2}$ J=3/2 ground state, with emission at 79.2 μm. Excitation to the $^2\Pi_{1/2}$ J=3/2 state by 53.3-μm photons can also contribute to the pump. If the transitions to and from the ground state (34.6, 53.3 and 79.2 μm) are optically thick, while those between the excited levels are optically thin, this scheme causes an inversion of the F=2/F=1 levels of the ground state, leading to 1612 MHz maser action. Another requirement is that there be sufficient 34.6- and/or 53.3-μm flux available: this is provided by continuum emission from dust in the outflow. Elitzur et al.'s proposed pumping mechanism had not been directly confirmed before the launch of ISO, because the OH rotational lines involved in this pumping scheme all occur at far-infrared wavelengths, between 34.6 and 163 μm, unobservable from the ground but accessible to ISO's spectrometers.

Sylvester et al. (1997) directly observed the OH pump line strengths in the ISO spectrun of the A-F hypergiant source IRC+10°420. The OH 34.6-μm doublet was confirmed to be in absorption in their SWS grating spectrum, while the lines in the resulting downward cascade (98.7, 163.2 and 79.2 μm; see Fig. 3) were all clearly detected in emission in the LWS spectrum, in agreement with predictions. Comparison of the observed photon absorption rate in the 34.6-μm doublet of 83×10^4 m^{-2} s^{-1} with observations made with the Nançay radiotelescope at the same epoch of a 1612 MHz maser line photon flux of

https://doi.org/10.1017/S0074180900203276 Published online by Cambridge University Press

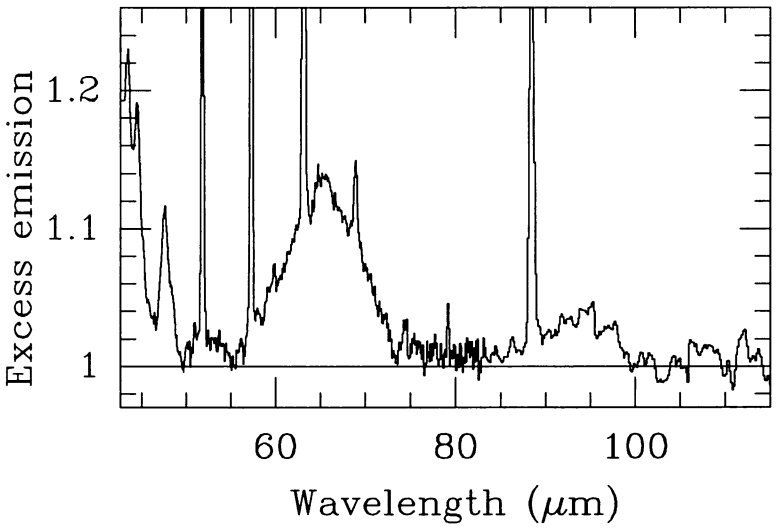

Figure 4. The LWS grating spectrum of NGC 6302 after background subtraction and division by a modified blackbody fit (45 K, $\lambda^{-1.2}$ emissivity) to the underlying continuum.

6.2 photons m^{-2} s^{-1}, implies a corresponding pumping efficiency of 7.5%. Since the 1612 MHz maser can also be pumped by radiative absorption by the 53.3 μm transition, as well as by radiative absorption and collisional excitation in the 79.2 μm line (see Fig. 3), a more appropriate estimate for the pumping efficiency comes from ratioing the emission rate in the 1612 MHz maser transition to that in the final downward pumping cascade line at 79.2 μm. The latter rate is measured to be $(200 \pm 30) \times 10^4$ m^{-2} s^{-1}, corresponding to an overall pumping efficiency for the 1612 MHz transition of IRC+10°420 of 3%. Similar observations of the M supergiant OH/IR source NML Cyg by the LWS consortium yield an overall pumping efficiency of 7%. The two measurements show good agreement with the predictions of Elitzur et al. (1976). Tung et al. (1998) have presented detailed modelling of the OH pumping conditions and maser radiative transfer for IRC+10°420, finding agreement with the observations of Sylvester et al.

6. Water ice emission bands in the IR spectra of cool evolved objects

The stretching-mode absorption band of water ice at 3.1 μm has been studied in the spectra of astronomical sources since the 1970's but, until the advent of ISO, the far-infrared ice bands had only been seen in the KAO spectra of a small number of sources (Omont et al. 1990), the most well known of which is IRAS 09371+1212 (the Frosty Leo Nebula; Forveille et al. 1987). The 3.1 μm band is only ever seen in absorption, because ice would evaporate before it could get hot enough to emit at 3 μm. Thus only water ice column densities in front of background infrared sources can be derived from observations of the optical depth in the 3.1 μm band. However, the lattice translational mode far-infrared

https://doi.org/10.1017/S0074180900203276 Published online by Cambridge University Press

bands of water ice can be observed in *emission*, so that the total emitting mass of ice can in principle be derived. Amorphous ice only exhibits a broad 44-μm band (transverse optical mode), whereas crystalline ice exhibits a narrow 44-μm band and a broader 62-μm peak (longitudinal acoustic mode). Thus the detection of the 62-μm peak requires the presence of crystalline ice (Omont et al. 1990; Moore et al. 1994).

Fig. 4 shows the LWS 43–197 μm grating spectrum of the Type I bipolar planetary nebula NGC 6302, after background subtraction and division by a modified blackbody fit to the underlying dust continuum (Lim et al., in preparation). A strong narrow emission feature is visible at about 43–44 μm. This was also seen at the long wavelength end of the SWS spectrum of NGC 6302 shown by Waters et al. (1996) and attributed by them to water ice and crystalline silicates. As noted above, this band can in principle arise from either amorphous or crystalline water ice. A strong, very broad emission feature (FWZI $\sim$ 15 μm) peaks at about 65 μm in the LWS spectrum of NGC 6302 (Fig. 4) and its presence implies that the ice is crystalline (there is also likely to be an underlying contribution by orthopyroxene to this feature). Laboratory measurements (e.g. Smith et al. 1994) show that the peak intrinsic strength of the 44-μm ice band is usually 2–3 times larger than that of the 62-μm band, whereas, from Fig. 4, it is clear that for NGC 6302 the peak strength of the 44-μm feature is less than 50% larger than that of the 65-μm feature. This can largely be explained by the fact that NGC 6302's low characteristic temperature of emission in this region ($\sim$45 K; see Fig. 4) shifts more emission into the longer wavelength band.

In addition to the two ice bands, the LWS spectrum of NGC 6302 in Fig. 4 exhibits several other emission features that are broader than the instrumental resolution of 0.3 μm. There is a band at 47.5 μm; a possible band at 52 μm (underlying the narrow [O III] 52-μm nebular emission line; this feature may be due to the longitudinal optical branch of crystalline ice; Bertie & Whalley 1967); and one at 69 μm, which is only slightly broader than the instrumental resolution, may be attributable to crystalline forsterite, Mg_2SiO_4 (see Waters & Molster, this volume). Finally, there is a very broad feature extending from 88–98 μm.

Barlow (1998b) has presented LWS spectra of a number of other sources that exhibit prominent 44- and 62-μm ice emission features, including those of the OH/IR star GL 5379, the O-rich post-AGB stars HD 101584 and HD 161796 and the young planetary nebula CPD–56°8032 (see Cohen et al., this volume, for a fuller discussion of the latter object). None of the O-rich AGB stars and M supergiants that show strong far-IR rotational line emission from H_2O have been observed to exhibit water ice bands, while none of the post-AGB objects that *do* show water ice band emission have been found to exhibit H_2O rotational lines. This is consistent with the scenario proposed by Omont et al. (1990) for the formation of crystalline water ice particles in the Frosty Leo Nebula (an O-rich post-AGB object), namely that water ice is only deposited onto silicate dust cores once the outflowing material has moved far enough out from the star for ambient temperatures to have dropped low enough for ice condensation to occur. While this process might well occur around AGB stars, warmer dust grains in the inner parts of their flows will dominate their overall spectra, whereas once strong mass loss has effectively ceased, after departure from the AGB, the absence of

warmer dust particles will render ice band emission more prominent, particularly if the final mass loss on the AGB had ratcheted up to superwind levels.

Acknowledgments. I would like to thank Drs. X.-W. Liu and R.J. Sylvester for their help in preparing several of the figures used here.

References

Aoki W., Tsuji T., Ohnaka K., 1998, A&A 333, L19

Barlow M.J., 1998a, Ap&SS 251, 15

Barlow M.J., 1998b, Ap&SS 255, 315

Barlow M.J., Nguyen-Q-Rieu, et al., 1996, A&A 315, L241

Bertie J.E., Whalley E., 1967, J. Chem. Phys. 46, 1271

Cernicharo J., 1998, Ap&SS 255, 303

Chen W., Neufeld D., 1995, ApJ 453, L99

Deguchi S., Nguyen-Q-Rieu, 1990, ApJ 360, L27

Elitzur M., Goldreich P., Scoville N., 1976, ApJ 205, 384

Forveille T., Morris M., Omont A., Likkel L., 1987, A&A 176, L13

Glassgold A.E., Huggins P.J., 1986, ApJ 306, 605

Haas M.R., Glassgold A.E., 1993, ApJ 410, L111

Haas M.R., Glassgold A.E., Tielens A.G.G.M., 1995, ASP Conf. Ser. 73, 397

Haniff C.A., Scholz M., Tuthill P.G., 1995, MNRAS 276, 640

Huggins P.J., Glassgold A.E., 1982, AJ 87, 1828

Justtanont K., de Jong T., et al., 1996, A&A 315, L217

Justtanont K., Feuchtgruber H., de Jong T., Cami J., Waters L.B.F.M., Yamamura I., Onaka T., 1998, A&A 330, L17

Moore H.H., Ferrante R.F., Hudson R.L., Nuth J.A., Donn B., 1994, ApJ 428, L81

Neufeld D.A., Chen W., et al., 1996 A&A 315, L237

Omont A., et al., 1990, ApJ 355, L27

Rodgers B, Glassgold A.E., 1991, ApJ 382, 606

Smith R.G., Robinson G., Hyland A.R., Carpenter G.L., 1994, MNRAS 271, 481

Sylvester R.J., 1998, in 'Solid Interstellar Matter - the ISO Revolution', ed. A.P. Jones, C. Joblin and L. d'Hendecourt, Editions Frontières, in press

Sylvester R.J., Barlow M.J., Skinner C.J., 1994, MNRAS 266, 640

Sylvester R.J., Barlow M.J., et al., 1997, MNRAS 291, L42

Thai-Q-Tung, Dinh-V-Trung, Nguyen-Q-Rieu, Bujarrabal V., Le Bertre T., Gérard E., 1998, A&A 331, 317

Truong-Bach, et al., Ap&SS 255, 325

Tsuji T., Ohnaka K., Aoki W., Yamamura I., 1997, A&A 320, L1

Tsuji T., Ohnaka K., Aoki W., Yamamura I., 1998, Ap&SS 255, 293

Waters L.B.F.M., et al., 1996, A&A 315, L361